Non-integer (or fractional) power model
of a viral spreading: application to the COVID-19

Alain Oustaloup[a], François Levron[b], Stéphane Victor[a,*], Luc Dugard[c]

[a]Univ. Bordeaux, CNRS, IMS UMR 5218, Bordeaux INP/ENSEIRB-MATMECA,
351 Cours de la Libération,
33405 Talence CEDEX, France
[b]Univ. Bordeaux, CNRS, IMB UMR 5251, Bordeaux INP/ENSEIRB-MATMECA,
351 Cours de la Libération,
33405 Talence CEDEX, France
[c]Univ. Grenoble Alpes, CNRS, Grenoble INP, GIPSA-Lab, 38000 Grenoble, France

Abstract

This paper proposes a very simple deterministic mathematical model, which, by using a power-law, is a *non-integer power model* (or *fractional power model (FPM)*). Such a model, in non-integer power of time, namely t^m up to constants, enables representing at each day, with a good precision, the totality of the contaminated individuals. Despite being enriched with knowledge through an internal structure based on a geometric sequence "with variable ratio", the model (in its non-integer representation) has only three parameters, among which the non-integer power, m, that determines on its own, according to its value, an aggravation or an improvement of the viral spreading. Its simplicity comes from the power-law, t^m, which simply expresses the singular dynamics of the operator of non-integer differentiation or integration, of high parametric compactness, that governs diffusion phenomena and, as shown in this paper, the spreading phenomena by contamination. The proposed model is indeed validated with the official data of Ministry of Health on the COVID-19 spreading. Used in prediction, it well enables justifying the choice of a lockdown, without which the spreading would have highly worsened. The comparison of this model in t^m with two known models having the same number of parameters, well shows that its representativity of the real data is better or more general. Finally, in a more fundamental context and particularly in terms of complexity and simplicity, a self-filtering action enables showing the compatibility between the *internal complexity* that the internal structure and its stochastic behavior present, and the *global simplicity* that the model in t^m offers in a deterministic manner: it is true that the non-integer power of a power-law is well a marker of complexity.

Keywords: COVID-19, viral spreading, modeling, prediction; fractional (or non-integer) power model (FPM), a FPM model as a convexity or concavity model; power-law, non-integer (or fractional) differentiation or integration, self-filtering internal structure.

1. Introduction

1.1. On our knowledge of the existing

The most common approach for modeling an epidemic is a behavior model, originally proposed by Kermack and McKendrick (1927). The population is divided into several categories and mathematical rules dictate how many people move from one category to another.

First, everyone is *Susceptible* (S) to become contaminated. Then some people become *Infected* (I) individuals who have been infected and are capable of infecting susceptible individuals. Finally, individuals, who have been infected enter the *Removed* (R) compartment, through either recovery or death. These SIR models can be improved by including *Exposed* (E) people but not yet contagious, leading to SEIR models. If post-recovery immunity is temporary, recovered people can go back

to S, thus leading to SEIRS models. The equations that determine how people move from one category to the next depend on a wide variety of parameters drawn from biology, behavior, politics, economy, weather, and more. Some of the extended SEIRS models can be found in Satsuma et al. (2004); Kwuimy et al. (2020); He et al. (2020); Ivorra et al. (2020); Dell'Anna (2020); Demongeot et al. (2020); Guan et al. (2020); Efimov and Ushirob (2020). Other extensions of the SEIRS models have been carried out by using fractional (or non-integer) order derivatives (Xu et al. (2020); Lu et al. (2020); Arfan et al. (2020)), as the non-integer operator is known to well model propagation phenomena such as biological systems, thermal diffusion systems, electro-chemical ones (fuel cells or batteries), etc.

Other kinds of spreading models exist in the literature to avoid sorting out people per categories, namely data-driven models. Black box models are used but the complexity and huge number of parameters render these models disconnected from reality and beyond understanding. On one hand, these models, as being more tied to data, can provide more accurate predictions in the short-term, but on the other hand no guarantee is proven for long-term predictions. Some data-driven mod-

*Corresponding author

Email addresses: `alain.oustaloup@ims-bordeaux.fr` (Alain Oustaloup), `f.levron@wanadoo.fr` (François Levron), `stephane.victor@ims-bordeaux.fr` (Stéphane Victor), `luc.dugard@gipsa-lab.grenoble-inp.fr` (Luc Dugard)

els use neural networks, deep learning, machine learning, YYG model[1], particle swarm optimization, etc. (see for example Liu et al. (2020); Huang et al. (2020); Zhao et al. (2020a); De-Leon and Pederiva (2020)).

Infection, death, and hospitalization numbers affect their usefulness not only as inputs for the model but also as outputs. The true number of infections is hard to evaluate when not everyone is tested. Deaths are countable, but they are the consequence of infections after some time delay. Therefore, other kinds of models have emerged by proposing transmission, networking and control measures to reduce the epidemic spreading such as the agent-based models, the sliding mode control (as governmental control input) (Rohith and Devika (2020)), mask wearing effects (Li et al. (2020)), human mobility control (Iacus et al. (2020)), lockdown effect, etc. (Huang and Qi (2020); De Visscher (2020); Atangana (2020); Tuan et al. (2020); Chen et al. (2020)).

Ferguson et al. (2005) have developed a stochastic model for the spread of infectious diseases, which also takes into account the geographic spreading. Simple models such as SEIRS ones are not sufficiently accurate to evaluate the spreading of an epidemic. There is a need for simple models that are sufficiently accurate for spreading predictions, so that quick and real-time decisions can be made on how to respond to epidemics. The Belgian Verhulst (1838) established a model of dynamical behavior of a population, named logistic growth model. Many studies use this model with three parameters for modeling the spreading of COVID-19 (Zhou et al. (2020); Kyurkchiev et al. (2020); Zhao et al. (2020b)). There are several possible generalizations of the Verhulst model such as proposed by Roosa et al. (2020) who give two well-known generalizations with four parameters: the generalized logistical growth model (Viboud et al. (2016); Ganyani et al. (2018)) and the generalized Richards model (Richards (1959); Wang et al. (2012); Wu et al. (2020)).

1.2. On the specific contributions of the article

The specific contributions of the article turn on a very simple deterministic mathematical model, in non-integer power of time, namely t^m up to constants, which enables representing, at each day, the totality of the contaminated individuals (which, from now on, will be named contaminated), with an absolutely satisfactory precision regarding the complexity of contamination phenomena. The model is characterized by three parameters, the non-integer power, m, as well as two constants, one being multiplicative of t^m and the other simply being additive. The non-integer power, m, determines on its own a viral spreading that worsens or gets better according to whether m is greater or lesser than one: indeed, the spreading graphical representation presents, for m greater than one, a convexity that expresses a spreading increasing more and more, therefore a viral aggravation ; while for m lesser than one, the curve presents a concavity that expresses a spreading increasing less and less, therefore a viral improvement.

The simplicity of the model in t^m (FPM) is due to the fact that t^m simply expresses a characteristic response, namely the

step response, therefore the dynamics, of the non-integer differentiation or integration operator. Applicable in real-time by means of Oustaloup's approximation (Oustaloup et al. (2000)), this operator is known for its parametric compactness and its capacity to govern complex phenomena (Oustaloup (1995, 2014)), including the diffusive phenomena and, as shown in this paper, the contamination spreading phenomena.

In order not to limit this model to a simple behavior model, it is enriched by knowledge (of countable nature) through an *internal structure*, in accordance with the daily recording of the new contaminated, and founded on a geometric sequence "with variable ratio", since the internal structure is none other than the sum of the $k + 1$ first terms of this sequence (sections 3 and 4). For each of the values of k, this sum achieves or synthesizes point by point (in this case day after day) a non-integer time function representing the evolution of the new contaminated number: this three parameter function (section 5) has the same form (therefore the same degree, m) as the model in t^m, even in its complete version that represents the evolution of the number of all the contaminated, new and former ones (section 5.5).

The internal structure, through which the model wins in knowledge, very simply enables formalizing the process of daily census of the new contaminated, and to represent day after day the whole of the new contaminated. To that effect, the internal structure is conceived for introducing ratios, q_k, between new contaminated between two consecutive days $k - 1$ and k (sections 3 and 4), then used without seeking to capture or represent the unpredictable, therefore the hazards of reality, in this case the random fluctuations of these ratios, which occur from day to day in reality given its complexity. Adopted for obvious reasons of simplicity, such a strategy is all the more justified as the fluctuations in question, besides interpretable as an internal noise, have only a negligible effect on the dynamics to be modelled, slower, as being expressed on several days. What follows is liable to precise the content of these words, and to reinforce the idea of not systematically seeking to represent the whole complexity of reality, particularly all these random fluctuations.

The internal structure of the model in t^m presents a remarkable property of filtering, through a *double effect* inherent to the form itself of the structure such as conditioned by the geometric sequence "with variable ratio", namely the sum of the products of the different ratios, $q_1, \ldots, q_k$ (sections 3 and 4):

- the first effect of filtering finds its cause in the terms of the sequence, that is to say the products of the different ratios, products that can filter by themselves the fluctuations of these ratios to only present residual fluctuations;

- the second effect of filtering finds its cause in the sum of the sequence terms, namely the non weighted sum of the products of the different ratios, a sum that therefore presents a (discrete) integral action that can filter at its turn the residual fluctuations of the products.

The specificity of such a property, that confers to the internal structure a *self-filtering* character with double effect, stands out by the joint effect of a sum and of products, thus overtaking

---

[1]https://covid19-projections.com developed by Youyang Gu

the filtering effect of a simple integrator, naturally limited to the one of a sum.

This *self-filtering double effect* is validated in section 5.4, through real curves (figure 8) which prove that the stochastic behavior due to the random fluctuations of the q_k, has globally no incidence or practically not, notably on the sum, s_k, of the new contaminated at day k. The modeling of this sum (or more precisely its result), which is an objective in epidemiology and then in this paper, therefore needs only a *deterministic model*, in this case the model in t^m, thus expressing the compatibility between *internal complexity* and *global simplicity*.

In other words, this self-filtering double effect liable to globally denoise the internal structure achieving (or synthesizing) the model in t^m, well expresses a coherent physical phenomenon, in the sense that the model in t^m is not noisy, even if it is noisy internally. This phenomenon assuredly is likely to remove the paradox between the simplicity of a model in t^m and the complexity of a noisy reality, thus reinforcing the interest of the parametric compactness of a model in t^m in the modeling of complex systems and phenomena (including among others those of finance (see Appendix B)).

2. A geometric sequence and the associated sum

Such as lead in this article, establishing a viral spreading model, calls, so it seems, a targeted mathematical recall as regards sequences, in order to better understand the geometric sequence "with variable ratio", introduced here so that the proposed model (via its internal structure) well represents the phenomenon of spreading by contamination.

In mathematics, a *sequence*, denoted $(u_k)_{k \geq 0}$, is written as the *sequence of terms*:

$$u_0, u_1, u_2, \ldots, u_k, \ldots;$$

of positive or null subscript k which indicates the rank, the *general term (of rank k)*, u_k, defines the sequence on its own.

Concerning the sum of the terms of the so defined sequence, in particular the first ones, the sum, s_k, of the $k + 1$ first terms of the sequence $(u_k)_{k \geq 0}$, is expressed according to the sum of terms:

$$s_k = u_0 + u_1 + \ldots + u_k.$$

For the most initiated ones, this sum s_k, associated with the sequence $(u_k)_{k \geq 0}$, is not without recalling the general term, s_k, of the *sequence* of the partial sums of the terms of $(u_k)_{k \geq 0}$, that defines the *series*, $(s_k)_{k \geq 0}$, knowing that *if a sequence is a sequence of terms, a series is a sequence of term sums.*

A *geometric sequence* (or *geometric progression*) is characterized by a *constant ratio*, q, between two consecutive terms, namely:

$$\frac{u_{k+1}}{u_k} = q \quad \forall k \geq 0 \quad \text{and} \quad u_0 \neq 0;$$

q is called *common ratio* of the sequence.

The term u_{k+1} with $k \geq 0$, can be written under the form of a *recurrence relation*, namely :

$$u_{k+1} = u_k q,$$

which expresses that each term of the sequence is the *product* of the precedent with the common ratio. Thus:

$$u_1 = u_0 q,$$
$$u_2 = u_1 q = u_0 q^2,$$
$$u_3 = u_2 q = u_0 q^3, \ldots,$$

the general term of the sequence then being:

$$u_k = u_0 q^k \quad \forall k \geq 0.$$

The sum s_k associated with the so defined geometric sequence, is given by the sum of terms:

$$s_k = u_0 + u_1 + \ldots + u_k \quad \text{with} \quad u_k = u_0 q^k,$$

namely, as one can show it:

$$s_k = u_0(1 + q + \ldots + q^k) = u_0 \frac{q^{k+1} - 1}{q - 1} \quad \text{for} \quad q \neq 1,$$

the case where $q = 1$ being trivial, as all the terms of the sequence, then being equal to u_0, immediately lead to $s_k = (k + 1)u_0$.

3. Geometric sequence with variable ratio and associated sum

In a simple geometric sequence, the common ratio is constant, in the sense that the ratio between two consecutive terms is the same whatever the rank k (as being independent of it), namely:

$$\frac{u_{k+1}}{u_k} = q \quad \forall k \geq 0 \quad \text{and} \quad u_0 \neq 0.$$

In the geometric sequence considered here, said "with variable ratio", the ratio is no more constant, in the sense that the ratio between two consecutive terms may be different according to rank k (as being dependent on it), *thus varying with the rank*, namely:

$$\frac{u_{k+1}}{u_k} = q_{k+1} \quad \forall k \geq 0 \quad \text{and} \quad u_0 \neq 0,$$

the term u_{k+1}, $k \geq 0$, being then defined by the recurrence relation:

$$u_{k+1} = u_k q_{k+1}.$$

Thus:

$$u_1 = u_0 q_1,$$
$$u_2 = u_1 q_2 = u_0 q_1 q_2,$$
$$u_3 = u_2 q_3 = u_0 q_1 q_2 q_3, \ldots,$$

the general term of the sequence then being:

$$u_k = u_0 q_1 \ldots q_k \quad \forall k \geq 1.$$

The sum s_k associated with the so defined geometric sequence "with variable ratio" , is given by the sum of terms:

$$s_k = u_0 + u_1 + u_2 + \ldots + u_k \quad \text{with} \quad u_k = u_0 q_1 \ldots q_k, k \geq 1,$$

3

namely:

$$s_k = u_0(1 + q_1 + q_1 q_2 + \ldots + q_1 \ldots q_k), k \geq 1.$$

By taking into account the *geometric means* $(\rho_1, \rho_2, \ldots, \rho_k, \ldots)$ of the different ratios $(q_1, q_2, \ldots, q_k, \ldots)$, it is then possible to write:

$$\rho_1 = q_1, \text{ mean of } q_1, \text{ namely } q_1,$$
$$\rho_2 = (q_1 q_2)^{1/2}, \text{ mean of } q_1 \text{ and } q_2,$$
$$\rho_3 = (q_1 q_2 q_3)^{1/3}, \text{ mean of } q_1, q_2 \text{ and } q_3,$$
$$\ldots,$$
$$\rho_k = (q_1 \ldots q_k)^{1/k}, \text{ mean of } q_1, \ldots, q_k,$$
$$\ldots,$$

from where one draws, by squaring, cubing, ... :

$$q_1 = \rho_1,$$
$$q_1 q_2 = \rho_2^2,$$
$$q_1 q_2 q_3 = \rho_3^3,$$
$$\ldots,$$
$$q_1 \ldots q_k = \rho_k^k$$
$$\ldots.$$

The terms of the sequence, expressed as functions of the different ratios, namely

$$u_0, \ u_0 q_1, \ u_0 q_1 q_2, \ \ldots, \ u_0 q_1 \ldots q_k, \ \ldots,$$

can then be expressed as functions of the geometric means of the different ratios, namely

$$u_0, \ u_0 \rho_1, \ u_0 \rho_2^2, \ \ldots, \ u_0 \rho_k^k, \ \ldots,$$

the sum s_k associated with this sequence, thus admitting an expression as a function of these means:

$$s_k = u_0 \left(1 + \rho_1 + \rho_2^2 + \ldots + \rho_k^k\right), \quad k \geq 1.$$

4. Why this kind of sequence with variable ratio

We have introduced this kind of sequence "with variable ratio", as well as the associated sum, in order to conceive a viral spreading model whose *internal structure* can be in conformity with the daily census process of the new contaminated.

In the census of the new contaminated by region and by day, that gives a space and time image of the spreading by contamination, there is no reason for the ratio of new contaminated between two consecutive days to be constant in time and therefore to be independent of the rank k. Indeed, the ratio between the new contaminated counted at day $k+1$ and the new contaminated counted at day k, assuredly depends on k, thus expressing that this ratio well varies day after day.

That amounts to saying that such a census cannot be formalized by a simple geometric sequence, which is with constant ratio, whereas it can be well formalized by a geometric

sequence "with variable ratio", whose ratio between two consecutive terms varies with the rank k.

Moreover, given the complexity of contamination phenomena, and particularly the stochastic aspects that highly contribute to this complexity, there is no reason for, day after day, the ratio of new contaminated between two consecutive days to increase or to decrease in a monotonic manner. It is indeed very likely that this kind of variation can be obtained in *mean*, in accordance with *smoothing* this ratio: hence, the geometric means of the different ratios, considered in our developments to go in this direction.

Such expectations, linked to our knowledge of complex phenomena, thus raise the points to be discussed, after confronting the proposed model to official data of the French Ministry of Health[2], which, from now on, will be named Ministry.

That being said, it is now possible to formalize the daily census process of the new contaminated, and this, of course, in conformity with the geometric sequence "with variable ratio" (in the case of a spreading aggravation):

- at day 0 (which corresponds to $k = 0$ in the sequence), the term of rank 0, u_0, represents the number of new contaminated individuals who have been counted this day;

- at day 1 (which corresponds to $k = 1$ in the sequence), the term of rank 1, u_1, greater than u_0, is the number of new contaminated individuals who have been counted this day, this number being written as $u_1 = u_0 q_1$, thus expressing that at day 1, there are q_1 times more new contaminated than the day before (day 0);

- at day 2 (which corresponds to $k = 2$ in the sequence), the term of rank 2, u_2, greater than u_1, is the number of new contaminated individuals who have been recorded this day, this number being written as $u_2 = u_1 q_2$, thus expressing that at day 2, there are q_2 times more new contaminated than at day 1;

- at day k, the term of rank k, u_k, greater than u_{k-1}, can be written as $u_k = u_{k-1} q_k$, thus expressing that at day k, there are q_k times more new contaminated than at day $k - 1$).

The sum s_k associated with the sequence, is written, as a function of the different ratios, according to

$$s_k = u_0 \left(1 + q_1 + q_1 q_2 + \ldots + q_1 \ldots q_k\right) \quad \text{for} \quad k \geq 1,$$

or, as a function of the geometric means of the different ratios, according to

$$s_k = u_0 \left(1 + \rho_1 + \rho_2^2 + \ldots + \rho_k^k\right) \quad \text{for} \quad k \geq 1.$$

This sum s_k, expressed by the one or the other of these two equations, represents the sum of the *new* contaminated who have been censed from day 0 to day k (0 and k included). The total sum of the contaminated at day k, is then obtained by adding the *former* contaminated before day 0.

---

[2]https://www.data.gouv.fr/fr/datasets/donnees-relatives-a-lepidemie-de-covid-19-en-france-vue-densemble/

5. Proposition and validation of a time model of viral spreading: the FPM model

Given that the non-integer differentiation or integration operator governs diffusion phenomena (thermal for example), one can legitimately suppose that this operator of non-integer order, $-m$ in differentiation or m in integration, with $m > 0$, and of step response in t^m (Appendix A and figure 1), also governs spreading phenomena by contamination. It is true that these phenomena, as the diffusion phenomena, fall under *complex phenomena*, for which the non-integer operator or its dynamics in power-law turn out to be particularly appropriated modeling tools, notably by the *parametric compactness* they offer in comparison with complexity. A newsworthy illustration that widens this context, incontestably lies in the field of huge networks and particularly of Internet network: Internet is indeed a paradigm of complex network, whose "degree distribution", which is inherent to the different average numbers of connections per node and which thus evokes a "diversity degree" (Oustaloup (2014)), follows a non-integer power law such as $N(k) = k^{-\gamma}$, $N(k)$ representing the number N of nodes endowed with k connections, and γ being a positive non-integer comprised between 2 and 3 (Santamaria (2017) and Mendes and da Silva (2009)). Other applicative fields in which the power-law dynamics occurs are presented in Appendix B.
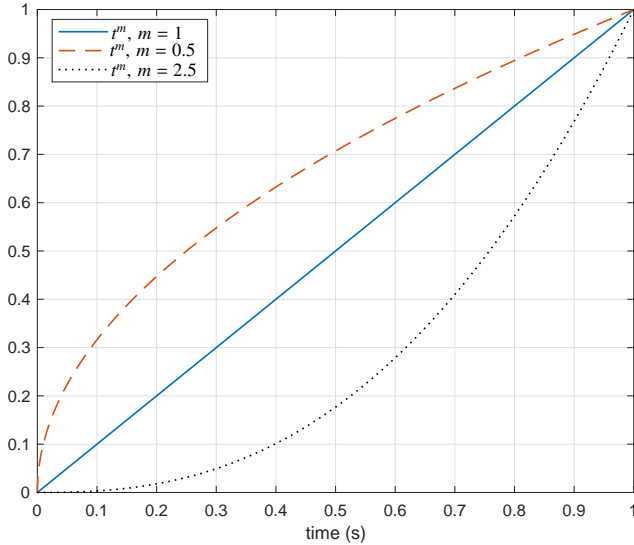

Figure 1: Step response in t^m, whose non-integer power, m, determines the curvature, namely a concavity for $m < 1$ and a convexity for $m > 1$: for $m \ll 1$, $t^m = e^{\ln t^m} = e^{m \ln t}$, is reduced to $1 + m \ln t$, whose variation in $\ln t$ is representative of a long memory phenomenon

To properly verify such an hypothesis of non-integer exponent, it suffices to directly check the conformity of a variation in t^m with the official data of Ministry, besides according to the comparative analysis presented further and which well confirms this conformity (section 6).

But it is possible to go beyond this direct verification, by determining the different ratios and the geometric means of the different ratios, inherent to the hypothesis of a variation in t^m,

and this, to see if, themselves, are well in conformity with the official data of the Ministry. This is a way to attempt to validate the internal structure proposed for the viral spreading model.

To that effect, a first step consists in imposing, to the sum of the new contaminated, s_k, a time variation in t^m (up to a multiplying constant and an additive constant), which amounts to simply writing, by introducing a positive constant, c:

$$s_k = u_0 \left(1 + ct^m\right),$$

namely, for $t = kh$ where h is the sampling period:

$$s_k = u_0 \left(1 + c(kh)^m\right),$$

therefore, given the expressions of s_k such as already determined:

$$u_0 \left(1 + q_1 + q_1 q_2 + \ldots + q_1 \ldots q_k\right) = u_0 \left(1 + c(kh)^m\right), \ k \geq 1$$

and

$$u_0 \left(1 + \rho_1 + \rho_2^2 + \ldots + \rho_k^k\right) = u_0 \left(1 + c(kh)^m\right), \ k \geq 1,$$

or, after simplifying by u_0 and 1:

$$q_1 + q_1 q_2 + \ldots + q_1 \ldots q_k = c(kh)^m \quad \text{with} \quad k \geq 1 \quad (1)$$

and

$$\rho_1 + \rho_2^2 + \ldots + \rho_k^k = c(kh)^m \quad \text{with} \quad k \geq 1. \quad (2)$$

From the two equations so obtained, a second step consists in determining the different ratios, q_1, q_2, ..., q_k, as well as the geometric means of the different ratios, ρ_1, ρ_2, ..., ρ_k, for a sampling period of one day, namely $h = 1$, and for the different values of k, namely 1, 2, 3, . . .

5.1. Determination of the different ratios

For $h = 1$, the first equation (1) becomes:

$$q_1 + q_1 q_2 + \ldots + q_1 \ldots q_k = ck^m \quad \forall k \geq 1.$$

For $k = 1$, a term by term identification immediately gives:

$$q_1 = c1^m = c.$$

For $k \geq 2$, let us rewrite the equation in conformity with:

$$q_1 + q_1 q_2 + \ldots + q_1 \ldots q_{k-1} + q_1 \ldots q_k = ck^m, \quad (3)$$

then let us replace k by $k - 1$:

$$q_1 + q_1 q_2 + \ldots + q_1 \ldots q_{k-2} + q_1 \ldots q_{k-1} = c(k-1)^m. \quad (4)$$

The difference of equations (3) and (4) leads to:

$$q_1 \ldots q_k = c \left(k^m - (k-1)^m\right), \quad (5)$$

or, by replacing k by $k - 1$:

$$q_1 \ldots q_{k-1} = c \left((k-1)^m - (k-2)^m\right), \quad (6)$$

5

the ratio of equations (5) and (6) then leading to:

$$q_k = \frac{k^m - (k-1)^m}{(k-1)^m - (k-2)^m} \quad \forall k \geq 2, \tag{7}$$

a result that expresses the general term of the sequence $(q_k)_{k \geq 2}$.

For $k >> 1$, it is convenient to write q_k under the form:

$$q_k = \frac{k^m - \left[k\left(1-\frac{1}{k}\right)\right]^m}{\left[k\left(1-\frac{1}{k}\right)\right]^m - \left[k\left(1-\frac{2}{k}\right)\right]^m}$$

$$= \frac{k^m - k^m\left(1-\frac{1}{k}\right)^m}{k^m\left(1-\frac{1}{k}\right)^m - k^m\left(1-\frac{2}{k}\right)^m},$$

or, by simplifying by k^m:

$$q_k = \frac{1 - \left(1-\frac{1}{k}\right)^m}{\left(1-\frac{1}{k}\right)^m - \left(1-\frac{2}{k}\right)^m},$$

namely, for k sufficiently high:

$$q_k \sim \frac{1 - \left(1-\frac{m}{k}\right)}{\left(1-\frac{m}{k}\right) - \left(1-\frac{2m}{k}\right)} = \frac{m/k}{m/k},$$

therefore, finally:

$$q_k \sim 1 \quad \forall k >> 1,$$

a result, not only remarkable of simplicity, but also very interesting with regard to the official data of the Ministry.

Figure 2 illustrates the variations of q_k given by (7) for different values of m ($m = 0.5$, 1.5 and 2.5).
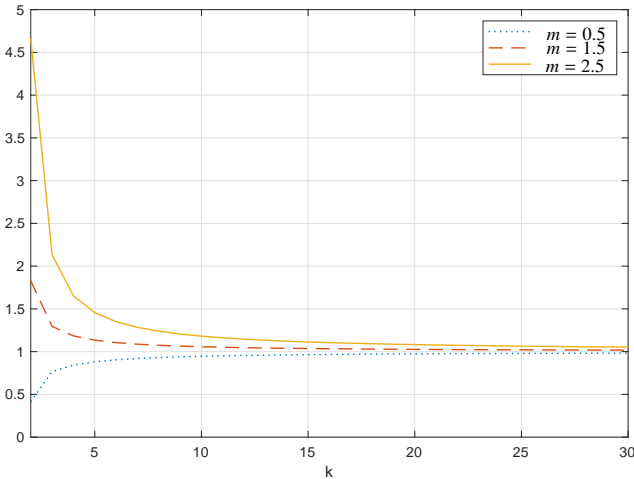

Figure 2: Variations of q_k versus k for three values of m

5.2. Determination of the geometric means of the different ratios

For $h = 1$, the second equation (2) becomes:

$$\rho_1 + \rho_2^2 + \ldots + \rho_k^k = ck^m \quad \forall k \geq 1.$$

For $k \geq 1$, let us rewrite this equation under the form:

$$\rho_1 + \rho_2^2 + \ldots + \rho_{k-1}^{k-1} + \rho_k^k = ck^m, \tag{8}$$

then let us replace k by $k-1$:

$$\rho_1 + \rho_2^2 + \ldots + \rho_{k-2}^{k-2} + \rho_{k-1}^{k-1} = c(k-1)^m. \tag{9}$$

The difference of equations (8) and (9) leads to:

$$\rho_k^k = c\,(k^m - (k-1)^m),$$

from where one draws:

$$\rho_k = \left(c^{\frac{1}{k}}\right)(k^m - (k-1)^m)^{\frac{1}{k}} \quad \forall k \geq 1, \tag{10}$$

a result that expresses the general term of the sequence $(\rho_k)_{k \geq 1}$.

For $k >> 1$, it is appropriated to write:

$$k^m - (k-1)^m = k^m - \left[k\left(1-\frac{1}{k}\right)\right]^m$$

$$= k^m - k^m\left(1-\frac{1}{k}\right)^m$$

$$= k^m\left[1 - \left(1-\frac{1}{k}\right)^m\right],$$

namely, for k sufficiently high:

$$k^m - (k-1)^m \sim k^m\left[1 - \left(1-\frac{m}{k}\right)\right] = k^m\frac{m}{k}.$$

ρ_k is then written:

$$\rho_k = \left(c^{\frac{1}{k}}\right)(k^m - (k-1)^m)^{\frac{1}{k}} \sim \left(c^{\frac{1}{k}}\right)\left(k^m\frac{m}{k}\right)^{\frac{1}{k}},$$

or:

$$\rho_k \sim \left(c^{\frac{1}{k}}\right)k^{\frac{m}{k}}\left(\frac{m}{k}\right)^{\frac{1}{k}}$$

$$= \left(c^{\frac{1}{k}}\right)\frac{k^{\frac{m}{k}}}{k^{\frac{1}{k}}}m^{\frac{1}{k}}$$

$$= (cm)^{\frac{1}{k}}\,k^{\frac{m-1}{k}},$$

or even, knowing that

$$k^{\frac{m-1}{k}} = e^{\ln\left(k^{\frac{m-1}{k}}\right)} = e^{\frac{m-1}{k}\ln k} = e^{(m-1)\frac{\ln k}{k}} :$$

$$\rho_k \sim (cm)^{\frac{1}{k}}\,e^{(m-1)\frac{\ln k}{k}},$$

or else, given that for k sufficiently high,

$$\frac{1}{k} \sim 0 \quad \text{and} \quad \frac{\ln k}{k} \sim 0 :$$

$$\rho_k \sim 1 \quad \forall k >> 1,$$

a result, not only remarkable of simplicity, but also very interesting with respect to the official data of the Ministry.

Figure 3 presents, for $c = 1$, the variations of ρ_k given by (10) for different values of m ($m = 0.5$, 1.5 and 2.5).
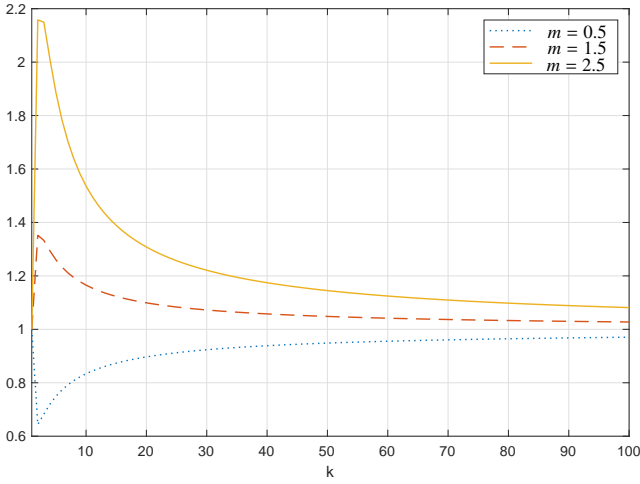
6

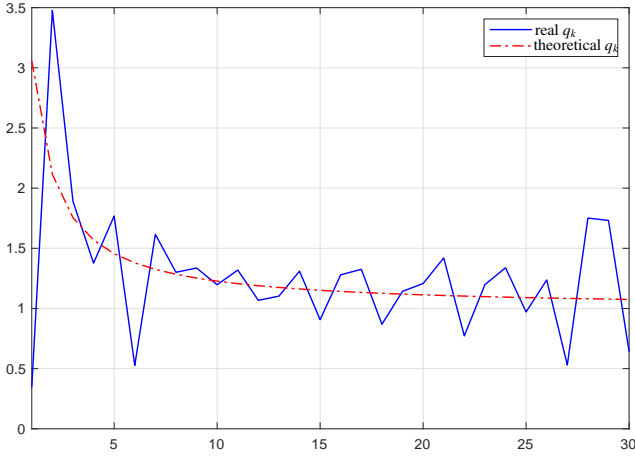Figure 3: Variations of ρ_k versus k for $c = 1$ and three values of m

Figure 4: Comparative illustration of the theoretical and real q_k for $m = 3.2523$: the theoretical q_k smooth the real q_k ; mean(E_r) = 0.0078

5.3. Validation of the internal structure of the model

The random fluctuations of the ratios, inherent to the reality complexity, are, properly, interpretable as fluctuations that are superimposed to a *smoothing* whose graphical representation is a curve representative, no more of the variations of these ratios, but of the variation mean.

So, the internal structure of the model in t^m, such as elaborated by disregarding the unpredictable, (therefore these random functions) can only represent the smoothing such as defined.

That is to say that the ratios q_k must be in conformity with the smoothing of the ratios stemming from the official data of Ministry. Thus, the validation of the proposed internal structure, can be carried out by the verification of this conformity.

But this verification can be reinforced by benefiting from the study of the geometric means ρ_k of the different ratios q_k, notably by comparing the geometric means obtained, theoret-
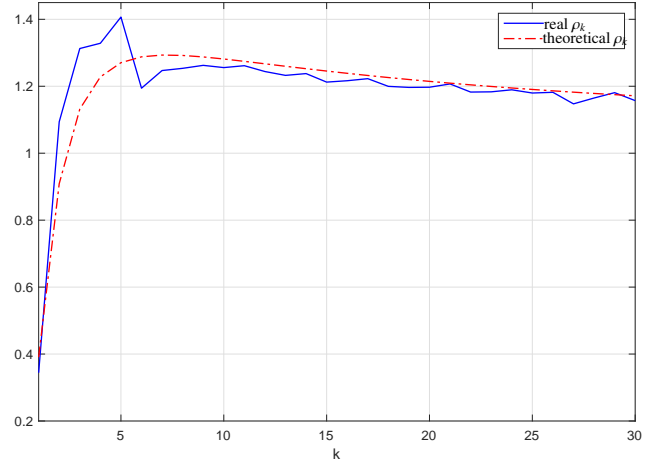

Figure 5: Comparative illustration of the theoretical and real ρ_k for $m = 3.2523$ and $c = 0.01497$: the theoretical ρ_k smooth the real ρ_k ; mean(E_r) = $-4.1497\,10^{-4}$

ically, with the internal structure and, really, with the official data of Ministry.

If a_k denotes the total number of contaminated counted at day k by the Ministry, the real q_k and ρ_k $\forall k \geq 1$, stemming from the official data, are computed in conformity with:

$$q_k = \frac{a_{k+1} - a_k}{a_k - a_{k-1}}$$

and

$$\rho_k = (q_1 \ldots . q_k)^{1/k},$$

where:

$$q_1 \ldots q_k = \frac{a_2 - a_1}{a_1 - a_0} \frac{a_3 - a_2}{a_2 - a_1} \ldots \frac{a_k - a_{k-1}}{a_{k-1} - a_{k-2}} \frac{a_{k+1} - a_k}{a_k - a_{k-1}}$$
$$= \frac{a_{k+1} - a_k}{a_1 - a_0}.$$

To evaluate the quality of the modeling, the maximum of the modulus of the absolute or relative errors, or the mean of the absolute or relative errors can be computed, namely (a_k being the real data and b_k the theoretical values stemming from the modeling):

$$\max\left(|E_a|\right) = \max\{|a_k - b_k|,\ 1 \leq k \leq n\}$$

or

$$\text{mean}\left(E_a\right) = \frac{1}{n} \sum_{k=1}^{n} (a_k - b_k)$$

or

$$\max\left(|E_r|\right) = \max\left\{\left|\frac{a_k - b_k}{b_k}\right|,\ 1 \leq k \leq n\right\}$$

or

$$\text{mean}\left(E_r\right) = \frac{1}{n} \sum_{k=1}^{n} \left(\frac{a_k - b_k}{b_k}\right).$$

To lead the verification of the conformity of q_k and ρ_k with the smoothing of the corresponding quantities stemming from
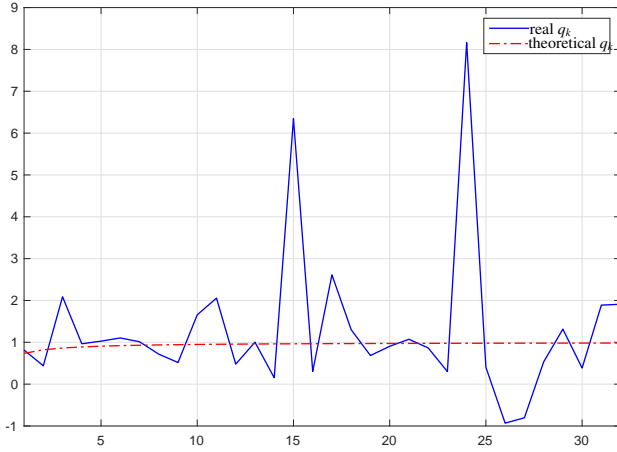
7

Figure 6: Comparative illustration of the theoretical and real q_k for $m = 0.4221$: the theoretical q_k smooth the real q_k ; mean(E_r) = 0.3591 because of the aberrations due to incorrect data
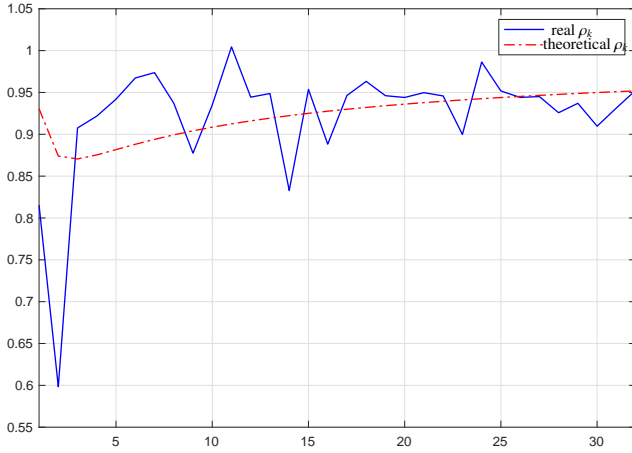

Figure 7: Comparative illustration of the theoretical and real ρ_k for $m = 0.4221$ and $c = 3.7202$: the theoretical ρ_k smooth the real ρ_k; mean(E_r) = 7.9843 10^{-5}

the official data, we have taken two values of m stemming from the identification, by the model in t^m, of the COVID-19 spreading in France (section 6): the first value of m, greater than 1, namely $m = 3.252$, corresponds to the convexity that period 1 presents, of 32 days, from March 1 to April 1 2020 ; the second value of m, less than 1, namely $m = 0.422$, corresponds to the concavity, that period 2 presents, of 34 days, from April 2 to May 5. Concerning the adjustment parameter, c, that takes part in the general expression of ρ_k, its determination according to the relation $c = B/u_0$ drawn from (12), is not pertinent in the sense that, if B is known (section 6), u_0 is known only through a noisy data: so, c is determined by optimization, so that the arithmetic mean of the absolute gaps, *mean(E_a)*, should be theoretically null. Thus, we get $c = 0.01497$ for period 1 (figure 5) and $c = 3.7202$ for period 2 (figure 7).

For the first values of k, figures 5 and 7 well show that the

geometric mean of noisy data is not a very significative mean. Note that the data can present some aberrations, particularly those collected at the weekend.

From the whole of the curves represented by figures 4 to 7, it turns out that the conformity to be verified is truly effective, thus validating the internal structure of the model in t^m, and consequently, the model itself (more precisely the model in t^m up to constants) as the internal structure is inherent to this model.

5.4. Validation of the self-filtering action of the internal structure of the model

The validation presented in the previous section 5.3 is enriched by the validation of the *self-filtering action* of the internal structure, such as described at the end of section 1.2 on the specific contributions of the article. This action, that makes the model in t^m not noisy even if it is internally noisy, indeed turns out to be graphically validated by figure 8, obtained with the real data of period 1 which corresponds to a convex growth.

The curves of this figure well convey two successive reductions of the random fluctuations of the ratios q_k between new contaminated between two consecutive days: it is, on one hand, a reduction between the q_k and the u_k (effect of a first filtering) and, on the other hand, a reduction between the u_k and the s_k (effect of a second filtering), the u_k denoting the new contaminated day after day, and the s_k denoting the daily sums of these new contaminated. Actually, through all these curves, figure 8 speaks by itself: indeed, this figure, which well illustrates two successive improvements of the signal-to-noise ratio, is sufficiently convincing for not being more commented.
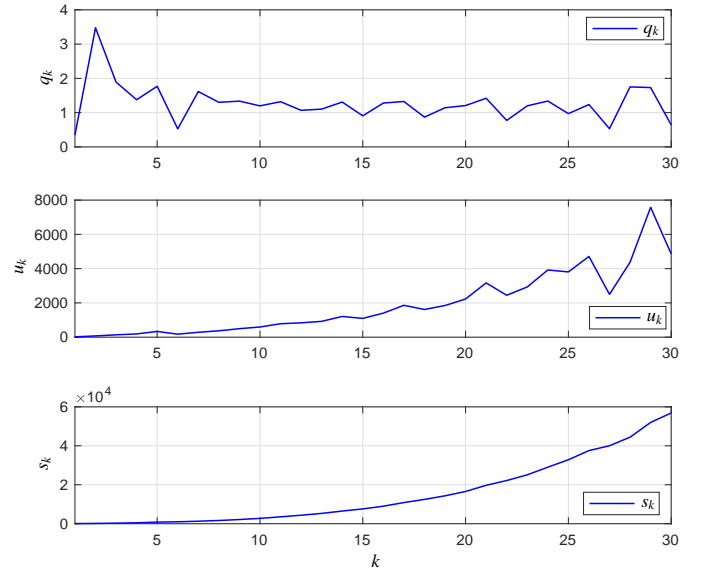

Figure 8: Illustration of the self-filtering action of the internal structure, from the real data, a_k, $k \geq 0$, corresponding to period 1. For $k \geq 1$: $q_k = (a_{k+1} - a_k)/(a_k - a_{k-1})$; $u_k = u_0 q_1 \ldots q_k = a_{k+1} - a_k$ with $u_0 = a_1 - a_0$; $s_k = u_0 + u_1 + \ldots + u_k$

8

The only comments are of another nature as they turn on the origin of the first filtering effect. At section 1.2, we have attributed this origin to the form of the sequence terms, therefore to the products of the different ratios, $q_1 \ldots q_k$, given the considered geometric sequence "with variable ratio". But if we had considered an arithmetic sequence "with variable difference", the origin of the first filtering would have been attributable to the sums of the different differences, $r_1 + \cdots + r_k$, stemming from the general term of the sequence, namely $u_k = u_0 + r_1 + \ldots + r_k$, $\forall k \geq 1$. These sums of differences, that present a discrete integral action, and which are thus likely to filter themselves the random fluctuations of the differences, offer an explanation, as or even more perceptible as the one founded on the geometric sequence "with variable ratio". Note that this sequence was preferred knowing that the q_k are always positive, contrary to the r_k.

Thus, more generally, for an internal structure based on a geometric or arithmetic sequence, its self-filtering property results from the form itself of the structure, which (in reality) globally eliminates the random fluctuations of its elements, thanks to the change from the *local* defined by the q_k or r_k, to the *global* defined by the s_k, namely the sums of the u_k. Such a property is admittedly likely to explain the compatibility between the *internal complexity* that the internal structure and its stochastic behavior present, and the *global simplicity* that the deterministic model offers through its power-law, t^m. But this simplicity form is not usual, in the sense that t^m presents, not only a mathematical structure remarkable of simplicity, but also a great richness by expressing very simply the complexity of reality, as if t^m, through its non-integer power m, *implicitly* had a complexity of another kind. Actually, the change to the global is accompanied by a transformation of the complexity nature: indeed, the internal complexity globally comes down to a non-integer power. It is true that the non-integer character of the power expresses or represents the complexity of systems and complex phenomena. That is to say that the non-integer power of a power-law is a marker of complexity. Given this context, it is convenient to recall that the power-law t^m is none other than the solution of a differential equation (Appendix A) whose non-integer order, m, expresses the character of infinite dimension (therefore the complexity) of the non-integer differentiation or integration operator, an operator which is itself (in the operational domain) a power-law, but of the operational variable, s.

5.5. A FPM model that takes into account the totality of the contaminated

After validating the internal structure inherent to the model in t^m, thus validating the model itself, it only remains to test the precision of this model, therefore its representativity, with the official data provided by the Ministry on the COVID-19 spreading. Knowing that these data relate to all the (new and former) contaminated, it is convenient to complete the model so that it represents the whole set of the contaminated, that is to say the total sum of contaminated at day k, S_k, resulting from the sum of new contaminated between days 0 and k, s_k, and the sum of the former contaminated before day 0, noted here C_f, namely:

$$S_K = s_k + C_f,$$

or, given the expression of s_k for $t = kh$ and $h = 1$:

$$S_k = u_0 (1 + ck^m) + C_f,$$

therefore, finally:

$$S_k = A + Bk^m, \tag{11}$$

with:

$$A = u_0 + C_f \quad \text{and} \quad B = u_0 c. \tag{12}$$

6. Time identification of the COVID-19 spreading by application of the FPM model to the official data on the contaminated

This section is dedicated to the time identification, by a non-integer model, of the COVID-19 spreading in France, based on data between March 1 and October 1 2020, namely on 7 months or 215 days.

More precisely, the identification method that uses the least squares, is founded on an *identification model* whose structure is given, namely

$$A + Bt^m, \tag{13}$$

and whose three parameters, to be determined in an optimal manner and without constraint, are respectively the additive constant, A, the multiplicative constant, B, and the non-integer exponent, m, which makes the specificity of the model.

The data of the Ministry on the total number a_i of the confirmed cases at day i, begin at March 1 2020 and are gathered in figure 9. This figure presents several time periods for which the curve form is different: the curve seems convex for the first 32 days, then concave for the following 33 days (from day 33 to day 66), then quasi-linear from day 67 to day 134, and finally convex. If the curve is convex, m is greater than 1: the daily number of confirmed new cases increases and the epidemic progresses. If the points (k, a_{d+k}) are aligned, then $m = 1$. If the curvature is concave, then $0 < m < 1$: the daily number of confirmed new cases decreases and the epidemic regresses. If the daily number of confirmed new cases is null, $m = 0$ and the epidemic stops.

For the period between days $d+1$ and $d+n$, where d denotes the day preceding this period and where n is the number of days of this period, a time modeling is sought under the form (13). That is to say that a_{d+k} is approximated by an expression of the form $A + Bk^m$ where k varies from 1 to n.

To that effect, the least squares are used to determine the three parameters $A > 0$, $B > 0$ and $m > 0$ that minimize the gap square sum. Given that the parameters A, B and m are calculated at best by optimization, on each period, the arithmetic mean of the absolute errors, $mean(E_a)$ is theoretically null. More precisely, if we operate with 20 significative digits, we find, for example, $mean(E_a) = -0.4\,10^{-13}$ for period 1, and $mean(E_a) = -0.10\,10^{-12}$ for period 2.
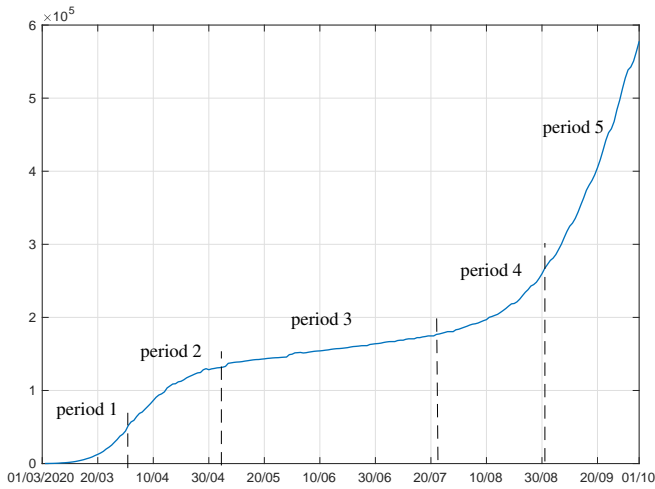
Figure 9: Evolution of the confirmed cases a_i between March 1 and October 1 2020, on 215 days

Figure 10: Comparative evolution, during period 1, of the contaminated recorded by the Ministry and obtained with the model in t^m:whereas mean(E_r) = −0.0618 on period 1 for all k, mean($E_r, k \geq 4$) = −0.0059, which conveys a precision lack of the model at the start (on 3 days) to the first growth phase of the pandemic, as commented in the case of figure 16

For period 1, between March 1 and April 1 2020, namely 32 days, where $d = 0$, $n = 32$ and $1 \leq k \leq 32$, the identification procedure leads to:

$$A = 434.8972; \quad B = 0.7148; \quad m = 3.2523.$$

For period 2, between April 2 and May 5 2020, namely 34 days, where $d = 32$, $n = 34$ and $1 \leq k \leq 34$, we get:

$$A = 30809.42; \quad B = 23934.54; \quad m = 0.4221.$$

For period 3, between May 6 and July 22 2020, namely 78 days, where $d = 66$, $n = 78$ and $1 \leq k \leq 78$, we get:

$$A = 136349.46; \quad B = 562.9646; \quad m = 0.9761.$$

For period 4, between July 23 and September 11 2020, namely 51 days, where $d = 144$, $n = 51$ and $1 \leq k \leq 51$, we get:

$$A = 183943.7; \quad B = 15.6681; \quad m = 2.3730.$$

For period 5, between September 12 and October 1 2020, namely 20 days, where $d = 195$, $n = 20$ and $1 \leq k \leq 20$, we get:

$$A = 363041.1; \quad B = 7300.427; \quad m = 1.13179.$$

The following figures, from 10 to 14, present, for each of the five periods so defined, the comparative evolution of the number of contaminated recorded by the Ministry and the number of contaminated obtained with the model in t^m.

7. On the prediction by the FPM model of the cases susceptible to be affected by the virus

The model in t^m which is used here as a predictor, is obtained, by identification, from the official data collected before the lockdown, notably between March 1 and March 16
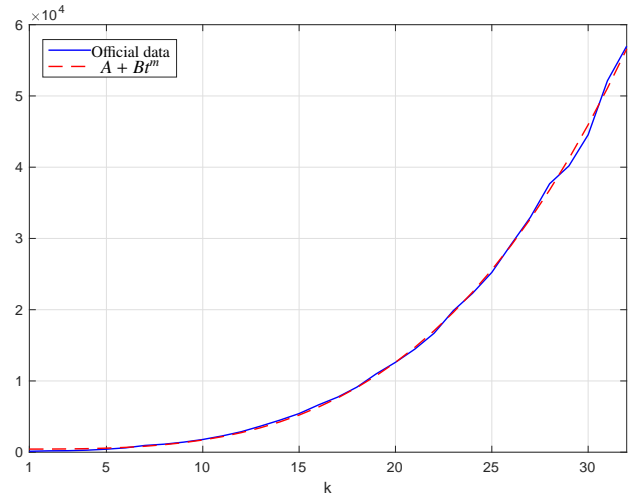
included, March 17 being the first day of the lockdown. The model parameters respectively admit for numerical values:

$$A = 205.2763; \quad B = 1.9419; \quad m = 2.9189.$$

Using this model until the last day of lockdown, May 10, enables comparing, during the lockdown, between March 17 and May 10 included, the evolution of the prediction and the one of the data provided by the Ministry (figure 15).

The comparison which is assessed on May 10, namely 492 274 cases predicted without the lockdown and 139 063 cases confirmed with the lockdown, turns out to be very eloquent in the sense that it well expresses the interest of the lockdown.

Concerning the precision associated with such a prediction, it is difficult to provide an estimation, as the prediction model is the subject of an exploitation that is demanding to say the least: indeed, it is established on a period limited to 16 days, whereas it is used with a prediction horizon of 55 days; the opposite would have been more in favor of the precision.

8. Comparison of the representativity of the FPM model and of two known models with three parameters

For a model, representativity (measured by the degree of representativity), is a characteristic that conveys the model capacity to represent reality. In this section, reality is materialized by the evolution of all the contaminated counted each day during period 1; the representativity of this reality is illustrated, in a comparative way, for the model in t^m and for two known models having also three parameters. If the model in t^m can be interpreted as a "convexity or concavity model", the two known models considered here can be interpreted as a "convexity model" for the one and as a "convexity and concavity model" for the other, a model that we have rewritten under a form in m^t, dual to the one of the model in t^m.
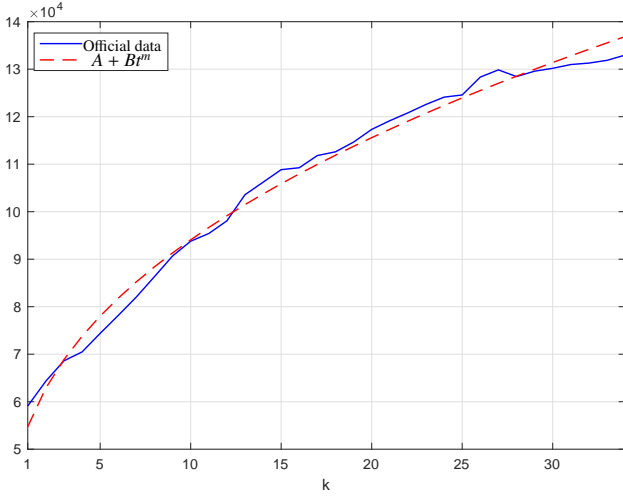
10

Figure 11: Comparative evolution, during period 2, of the contaminated recorded by the Ministry and obtained with the model in t^m: mean(E_r) = $1.5731 \, 10^{-4}$

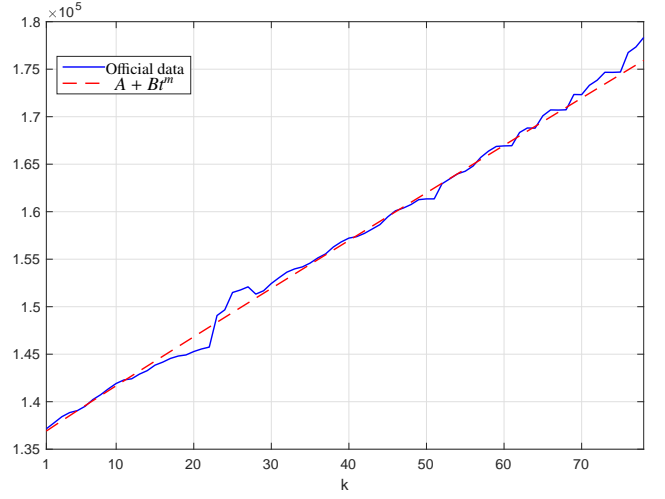Figure 12: Comparative evolution, during period 3, of the contaminated recorded by the Ministry and obtained with the model in t^m: mean(E_r) = $9.4442 \, 10^{-4}$

8.1. The model of Verhulst: a convexity and concavity model (or sigmoid model)

Taking into account a convex then concave growth, the Verhulst model and its generalizations are liable to represent, both first and second growth phases of the epidemics.

Around 1838, the Belgian P.F. Verhulst (Verhulst (1838, 1845)) has established a model of dynamical behavior of a population, named logistic growth model. If a_k is the size of the population at day k, for $k \geq 0$, the growth rate of this population at day $k + 1$ is $(a_{k+1} - a_k)/a_k$.

This rate is equal to the difference between the birth rate and the death rate at day k. Assuming that the daily birth rate and daily death rate are affine functions of the population size, it then comes:

$$\frac{a_{k+1} - a_k}{a_k} = N(a_k) - M(a_k),$$

with:

$$N(x) = n_1 + n_2 x \quad \text{and} \quad M(x) = m_1 + m_2 x.$$

This expression is none other than the discretization of a time differential equation in $f(t)$, where $f(k) = a_k$, namely:

$$f'(t) = f(t) \left[N\left(f(t)\right) - M\left(f(t)\right) \right] \quad \text{with} \quad f(0) = a_0,$$

a differential equation in which:

$$N\left(f(t)\right) = n_1 + n_2 f(t) \quad \text{and} \quad M\left(f(t)\right) = m_1 + m_2 f(t),$$

therefore:

$$f'(t) = f(t) \left[n_1 - m_1 + (n_2 - m_2) f(t) \right],$$

or:

$$f'(t) = (n_1 - m_1) f(t) \left[1 - \frac{m_2 - n_2}{n_1 - m_1} f(t) \right],$$

or even:

$$f'(t) = a f(t) \left[1 - \frac{f(t)}{K} \right],$$

by posing

$$a = n_1 - m_1 \quad \text{and} \quad K = \frac{n_1 - m_1}{m_2 - n_2} = \frac{a}{m_2 - n_2}.$$

The solution of this differential equation, $f(t)$, admits an expression with three parameters, K, a_0 and a:

$$f(t) = \frac{K}{1 + \left(\frac{K}{a_0} - 1\right) e^{-at}}, \tag{14}$$

an expression which is easier to verify than to establish. It is true that to verify it, it suffices to differentiate $f(t)$ after writing it under the form $f(t) = K/D(t) = K D^{-1}(t)$, namely

$$f'(t) = \frac{Ka}{D^2(t)} \left(\frac{K}{a_0} - 1\right) e^{-at} = a \frac{f(t)}{D(t)} \left(\frac{K}{a_0} - 1\right) e^{-at},$$

then to express $f'(t)$ versus $f(t)$, by using

$$\frac{1}{D(t)} = \frac{f(t)}{K} \quad \text{and} \quad \left(\frac{K}{a_0} - 1\right) e^{-at} = \frac{K}{f(t)} - 1,$$

to which case:

$$f'(t) = a f(t) \left[1 - \frac{f(t)}{K} \right].$$

In the case of an epidemic, $f(t)$ represents the number of contaminated cases at instant t.

8.2. Use and generalization of Verhulst model

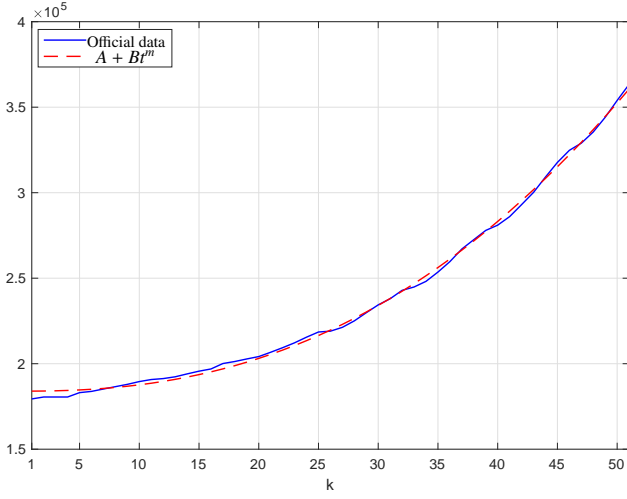Many articles use this model with three parameters for the COVID-19.

11

Figure 13: Comparative evolution, during period 4, of the contaminated recorded by the Ministry and obtained with the model in t^m: mean(E_r) = $-6.4613\,10^{-4}$

Zhou et al. (2020) use the differential equation:

$$P'(t) = rP(t)\left(1 - \frac{P(t)}{K}\right),$$

and its solution:

$$P(t) = \frac{KP(0)e^{rt}}{P(0)(e^{rt} - 1) + K}.$$

Kyurkchiev et al. (2020) use a model of the form:

$$y(t) = \frac{r}{1 + e^{a_0 + a_1(t)}},$$

which is analogous to Verhulst model and is generalized to:

$$y(t) = \frac{r}{1 + e^{a_0 + a_1 t + a_2 t^2 + \ldots}}.$$

Zhao et al. (2020b) use the model:

$$f(t) = \frac{af(0)}{bf(0) + (a - bf(0))e^{at}}.$$

Rémond and Rémond (2020) use the model:

$$E(t) = \frac{L}{1 + e^{-k(t-\tau)}}.$$

There are several possible generalizations of Verhulst model such as proposed by Roosa et al. (2020) who give two well-known generalizations with four parameters:

- the generalized logistic model (GLM), namely

$$\frac{dC(t)}{dt} = rC(t)^p\left(1 - \frac{C(t)}{K}\right),$$

used, among others, by Viboud et al. (2016) and Ganyani et al. (2018), the four parameters being r, p, K and $C(0)$;
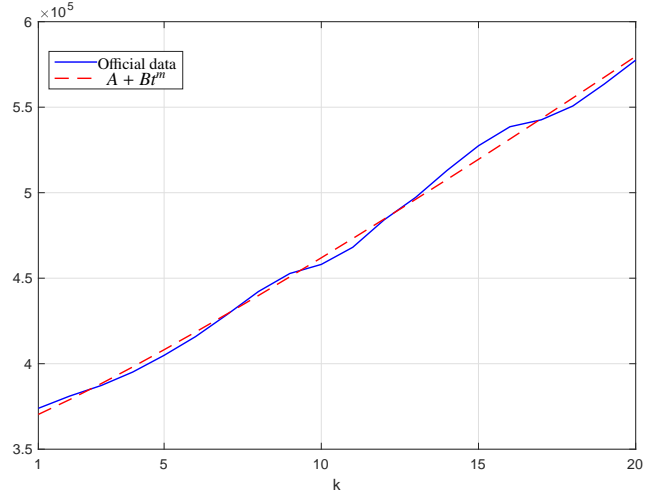

Figure 14: Comparative evolution, during period 5, of the contaminated recorded by the Ministry and obtained with the model in t^m: mean(E_r) = $7.9843\,10^{-5}$

- the Richards model, namely

$$\frac{dC(t)}{dt} = rC(t)\left(1 - \left(\frac{C(t)}{K}\right)^a\right),$$

used, among others, by Wang et al. (2012) and Richards (1959) in 1959, the four parameters being r, a, K and $C(0)$.

Richards model is found under a generalized form with five parameters, called generalized Richards model (GRM), namely (Wu et al. (2020)):

$$\frac{dC(t)}{dt} = rC(t)^p\left(1 - \frac{C(t)^a}{K}\right),$$

the five parameters being r, p, a, K and $C(0)$, with $p \in [0, 1]$.

8.3. A convexity model

The model presented in this section is used to represent the first growth phase of the epidemics. Its use is indeed kept for convex growths.

By only taking the first factor of the GLM and GRM models, these models are reduced to a same model such as presented in Wu et al. (2020), Viboud et al. (2016) and Tolle (2003), namely:

$$\frac{dC(t)}{dt} = rC(t)^p \quad \text{with} \quad r > 0 \text{ and } p \in [0, 1], \qquad (15)$$

a differential equation that defines a model with three parameters, r, p and $C(0)$, and that admits three different solutions according to whether $p = 0$, $p = 1$ or $0 < p < 1$: an affine solution for $p = 0$, an exponential solution for $p = 1$ or a sub-exponential solution for $0 < p < 1$.

If for $p = 0$, the solution is of constant slope, r, as $C(t) = rt + C(0)$, for $p = 1$, the differential equation then being linear, its solution is here the one of a system of first order, namely:
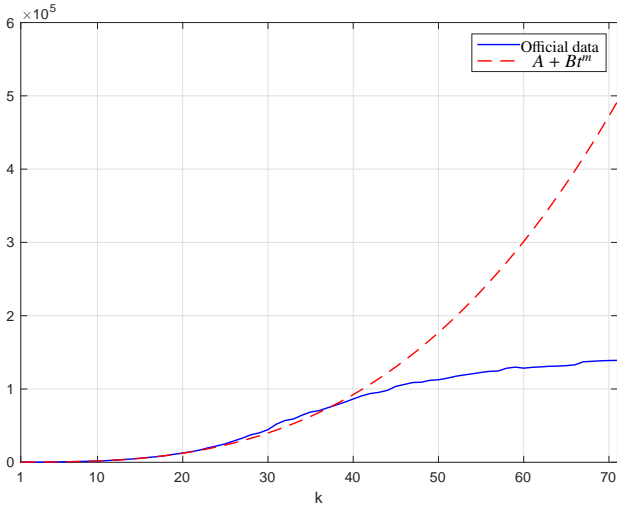
$$C(t) = C(0)e^{rt}.$$

Figure 15: Comparative evolution, during the lockdown, of the model prediction and the data provided by the Ministry

For $0 < p < 1$, the differential equation then being nonlinear, the establishment of its solution requires a rewriting of the equation in conformity with:

$$C(t)^{-p}C'(t) = r,$$

namely, given the formula

$$u(t)^{\alpha}u'(t) = \left(\frac{u(t)^{\alpha+1}}{\alpha+1}\right)' \quad \forall u(t) \text{ and } \forall \alpha \neq -1:$$

$$\left(\frac{C(t)^{1-p}}{1-p}\right)' = r,$$

therefore:

$$\left((C(t)^{1-p}\right)' = r(1-p),$$

or, by integrating, thus introducing an integration constant C:

$$C(t)^{1-p} = r(1-p)t + C,$$

or even:

$$C(t) = (r(1-p)t + C)^{\frac{1}{1-p}},$$

or else, knowing that

$$C(0) = C^{\frac{1}{1-p}} \quad \text{hence} \quad C = C(0)^{1-p}:$$

$$C(t) = \left(r(1-p)t + C(0)^{1-p}\right)^{\frac{1}{1-p}},$$

a solution with non-integer exponent, that we rewrite here under a form comparable to the one of the model in t^m, $A + Bt^m$, namely:

$$C(t) = (A' + B't)^{m'},$$

with:

$$A' = C(0)^{1-p}, \quad B' = r(1-p)$$

and

$$m' = \frac{1}{1-p} > 1 \quad \text{as} \quad 0 < p < 1.$$

Given the two model structures, if the model in t^m can be interpreted as a "model with explicit power of time", the other model can be interpreted as a "model with implicit power of time", a power which is non-integer for both models.

Let us express the derivatives of order 1 and 2 of both models in question:

- for the model $C(t) = A + Bt^m$,

$$C'(t) = mBt^{m-1}$$

  and

$$C''(t) = m(m-1)Bt^{m-2};$$

- for the model $C(t) = (A' + B't)^{m'}$,

$$C'(t) = m'B'(A' + B't)^{m'-1}$$

  and

$$C''(t) = m'(m' - 1)B'^2(A' + B't)^{m'-2}.$$

If all parameters are considered positive, it is then possible to write:

- for the first model,
  $C'(0) = 0$ for $m > 1$ and $C'(0) = \infty$ for $0 < m < 1$, null or infinite initial slope,
  $C'(t) > 0$, increasing $C(t)$,
  $C''(t) > 0$ for $m > 1$, increasing $C'(t)$ according to a convexity of $C(t)$,
  $C''(t) < 0$ for $0 < m < 1$, decreasing $C'(t)$ according to a concavity of $C(t)$;

- for the second model,
  $C'(0) = m'B'A'^{m'-1} > 0$, positive initial slope,
  $C'(t) > 0$, increasing $C(t)$,
  $C''(t) > 0$ for $m' > 1$, increasing $C'(t)$ according to a convexity of $C(t)$,
  $C''(t) < 0$ for $0 < m' < 1$, decreasing $C'(t)$ according to a concavity of $C(t)$.

Even if the model represented by the differential equation (15) imposes, on its solution $C(t)$, an exponent m' greater than 1, we have wished to find out more, by studying this solution for an exponent m' comprised between 0 and 1, which corresponds to $p < 0$ for the differential equation and its solution.

Thus, to lead a comparative study between the parameters of both models for m and m' comprised between 0 and 1, and this for simply understanding why the "convexity model" is not proposed for concave growths, it is convenient to approximately express A' and B' versus A, B, m and m' by considering the identity of the models at an initial instant, $t = 0$, and at a final instant, $t = t_n$, then to analyze A' and B' for the small values of m'.

Let be the two models, denoted here by $C_1(t)$ and $C_2(t)$:

$$C_1(t) = A + Bt^m, \quad \text{with} \quad A, B > 0 \quad \text{and} \quad 0 < m < 1,$$

and

$$C_2(t) = (A' + B't)^{m'}, \quad \text{with} \quad A', B' > 0 \quad \text{and} \quad 0 < m' < 1.$$

13

For $t = 0$:

$$C_1(0) = A \quad \text{and} \quad C_2(0) = A'^{m'},$$

then, given that $C_1(0) = C_2(0)$:

$$A' = A^{\frac{1}{m'}}. \tag{16}$$

For $t = t_n$:

$$C_1(t_n) = A + Bt_n^m \quad \text{and} \quad C_2(t_n) = (A' + B't_n)^{m'},$$

then, given that $C_1(t_n) = C_2(t_n)$:

$$A' + B't_n = (A + Bt_n^m)^{\frac{1}{m'}},$$

from where one draws:

$$B' = t_n^{-1}\left[(A + Bt_n^m)^{\frac{1}{m'}} - A^{\frac{1}{m'}}\right],$$

namely, by posing

$$Btn^m = \alpha A \quad \text{with} \quad \alpha > 0 :$$

$$B' = t_n^{-1}A^{\frac{1}{m'}}\left[(1 + \alpha)^{\frac{1}{m'}} - 1\right]. \tag{17}$$

Given that A, α and m' are positive, the relations (16) and (17) well show that A' and B' tend towards infinity when m' tends towards zero. This phenomenon is in conformity with the huge values of A' and B' that we have obtained, even for $m' = 0.308$ which is far from zero, in the case of an identification attempt of the second period with m' between 0 and 1. Indeed, whereas $A = 30809.42$ and $B = 23934.54$ (m being 0.422), the values of A' and B' reach respectively, for a similar precision, $A' = 0.106\,10^{16}$ and $B' = 0.123\,10^{16}$ (for $m' = 0.308$).
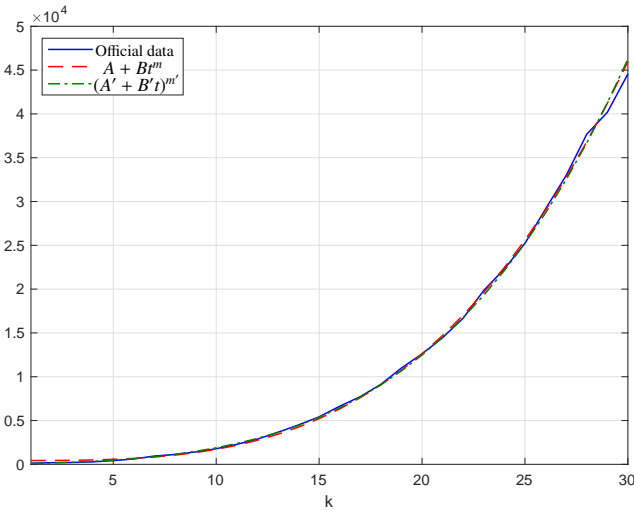

Figure 16: Comparative evolution, during period 1, of the contaminated recorded by the Ministry, and obtained with the model in t^m, $C_1(t)$, and the "convexity model", $C_2(t)$, such that $A' = 2.5883$, $B' = 0.3125$, and $m' = 4.3281$: for $C_1(t)$, mean$(E_r, k \geq 1) = -0.0618$, mean$(E_r, k \geq 4) = -0.0059$, max$(|E_a|, k = 30) = 1406$; for $C_2(t)$, mean$(E_r, k \geq 1) = 0.0042$, mean$(E_r, k \geq 4) = -0.0098$, max$(|E_a|, k = 30) = 1709$

Such a numerical explosion of the parameters for low values of m', therefore well illustrates the difficulty of the model $C_2(t)$ to naturally capture the concave growths.

On the other hand, for a convex growth such as the one for period 1, the model $C_2(t)$, with $m' > 1$, is absolutely representative of the evolution of official data corresponding to this period. Indeed, figure 16 seems to show that the model $C_2(t)$ is, for a convexity, as representative as the model $C_1(t)$. More precisely, with respect to the latter, it offers a comparable precision to say the least, since its precision is better at the start (on three days) and similar beyond, as shown, with more nuance, by the numerical errors associated with figure 16.

Appropriated to the representation of the complexity that involves high numbers of cases, the model in t^m does not have the vocation to represent small numbers of cases inherent to the short times: in other words, in reality, where the non-integer operator has only a sense at medium frequencies, the power-law dynamics, t^m, has only a sense at medium times, therefore beyond the short times. Besides, in the real case of the epidemic start, the nil slope of the initial behavior of t^m, is not stranger to the representativity lack of the FPM model at the short times.

As for the precision of the FPM model in relation to the number of cases, it can be illustrated with the confirmed cases of the COVID-19 in Switzerland, given that these ones have been provided from a first case, recorded on February 25 2020. Between week 1 starting at this date with one confirmed case, and week 10 starting at April 28 2020 with 29264 confirmed cases, the maximum of the relative errors goes from 0.816 to 0.000976, by taking the intermediate values 0.321 and 0.0164 for the weeks 2 and 5. That is to say that the precision is clearly improved by the case number (therefore by complexity).

8.4. Rewriting of Verhulst model under the form of a model in m^t whose properties are presented

The Verhulst model (14) admits an immediate rewriting:

$$f(t) = \frac{K}{1 + \frac{K-a_0}{a_0}e^{-at}},$$

or, by multiplying the numerator and the denominator by $a_0/(K - a_0)$:

$$f(t) = \frac{\frac{Ka_0}{K-a_0}}{\frac{a_0}{K-a_0} + (e^{-a})^t},$$

namely, by posing

$$A = \frac{Ka_0}{K - a_0}, \; B = \frac{a_0}{K - a_0} \quad \text{and} \quad m = e^{-a} :$$

$$f(t) = \frac{A}{B + m^t},$$

a model in m^t, with three parameters, A, B and m, dual to the model in t^m, $A + Bt^m$.

Used as an identification model, the function

$$f(t) = \frac{A}{B + m^t},$$

is applied in a time interval such that $1 \leq t \leq n$.

14

This function is a particular solution of the differential equation

$$f'(t) = -\ln(m)\left(f(t) - Bf^2(t)/A\right), \; f(1) = A/(B + m).$$

Its derivative is

$$f'(t) = \frac{-A\ln(m)m^t}{(B + m^t)^2}.$$

The function $f(t)$ is increasing if $A > 0$ and $0 < m < 1$, or if $A < 0$ and $m > 1$, and decreasing otherwise.

Its second derivative is

$$f''(t) = \frac{A\ln(m)m^t(m^t - B)}{(B + m^t)^3}$$

$f(t)$ can have an inflexion point in t_0 if $f''(t_0) = 0$. This is only possible if $t_0 = \frac{\ln B}{\ln m}$ and if, moreover, $1 < t_0 < n$.

Such a t_0 exists if $0 < B < 1$ and $0 < m < 1$, or if $B > 1$ and $m > 1$.

If $0 < B < 1$ and $0 < m < 1$, then $1 < t_0 < n$ if $m^n < B < m$.

If $B > 1$ and $m > 1$, then $1 < t_0 < n$ if $m < B < m^n$.

If t_0 is not between 1 and n, then $f(t)$ is concave or convex if t varies from 1 to n.

If t_0 is between 1 and n, then the curve of $f(t)$ is a sigmoid, with two convex and concave parts.

8.5. Determination and application of the model in m^t

Given a finite sequence (a_k), k varying from 1 to n, where a_k is a daily epidemic datum, and the model in m^t with three parameters, $f(A, B, m, t)$, these parameters need to be calculated so that $b_k = f(A, B, m, k)$ is as close as possible to a_k, for all k between 1 and n.

Even if the model in m^t is a fraction, the calculus can be simply carried out by minimizing the square sum of the absolute errors such as:

$$E(A, B, m) = \sum_{k=1}^{n}\left(a_k\left(B + m^k\right) - A\right)^2.$$

To minimize $E(A, B, m)$, it suffices to cancel the partial derivatives with respect to these three parameters.

So determined, the model in m^t is now applied, as an identification model, to period 1 which is the beginning of the epidemic in France. This application leads to the following numerical values:

$$A = 107.9402; \; B = 0.0022803; \; m = 0.7642119.$$

Whereas period 1 presents a convexity, the value of B belongs to an interval corresponding to an inflexion point, thus expressing that the model in m^t is here inappropriate, as figure 17 shows it.

In conclusion, figure 17 conveys an eloquent result: the comparative illustration of the representativity of the models in t^m and m^t, clearly proves to be in favor of the model in t^m. But this drawback of the model in m^t is due to its strategy requirement, in the sense that this model aims, with a unique parameterization, to represent both convex and concave phases of the epidemic growth.
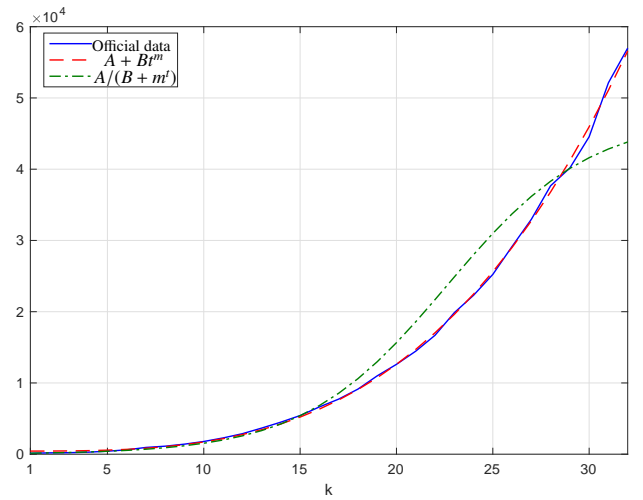

Figure 17: Comparative evolution, during period 1, of the contaminated recorded by the Ministry and obtained with the models in t^m and m^t: the comparison well illustrates the representativity difference of the models

9. Conclusion

This paper develops an original approach of a very simple deterministic model with three parameters, the FPM model. The non-integer power of time (significative to the curvature of the viral spreading evolution), enables representing at each day the totality of the contaminated, and the internal structure, founded on a geometric sequence "with variable ratio", enables, on one hand, to formalize the daily censing of the new contaminated and, on the other hand, to represent day after day the whole of the new contaminated.

The simplicity of the model is due to its variation in t^m which is a response to the non-integer differentiation or integration operator, an operator known for its capacity to simply represent complex phenomena such as diffusion phenomena (of thermal origin (Battaglia et al. (2000)) or fluidic one (Oustaloup (2014))).

Founded on a known structure and unknown parameters, q_k, to be determined, the construction point by point of a non-integer time function of the same form as the model in t^m, can be interpreted as a *time synthesis* in non-integer. This synthesis is not without evoking an analogy with the *frequency synthesis* of the non-integer differentiation or integration operator, from a synthesis network having a known structure and unknown parameters to be determined. Whilst there is indeed an analogy through a common context of synthesis, this analogy ends here, in the sense that both syntheses in question are not of the same nature. On one hand, the first synthesis turns on a time response of a non-integer operator, while the second one turns on the frequency response of the operator itself. On the other hand, the first synthesis uses an evolutive structure of synthesis, due to an *evolutive dimension* that increases with time, whereas the second one uses a fixed structure of synthesis with a fixed given dimension.

The model internal structure is conceived so as to introduce ratios likely to represent those of the new contaminated

15

between two consecutive days, then used without seeking to represent the unpredictable inherent to reality hazards, particularly the random fluctuations of these ratios. It is true that, as shown in the paper, these fluctuations have a negligible effect on the slower dynamics to be modelled by the model in t^m, and this, because of the self-filtering character of the internal structure, highlighted through a filtering double effect. More generally, this self-filtering character removes the paradox between the simplicity of a model in t^m and the reality complexity, thus consolidating the interest of this type of model in modeling complex systems and phenomena.

Finally, if for the sake of simplicity, the model internal structure only represents the reality mean day after day, namely an "averaged reality", this average proves to be sufficient. Indeed, on one hand, it is in conformity with the model in t^m which, on the other hand, is in conformity with reality it is supposed to represent, being well representative of this reality. These words, whose content deserves some thinking and some hindsight, are largely validated by a comparative study of a set of graphics, whose curves are obtained, in practice, with the official data of Ministry and, theoretically, with the internal structure (equations (7) and (10)) then with the model in t^m (equation (13)).

Used as a prediction model, to predict the number of cases liable to be affected by the virus, this model highly justifies the lockdown choice, without which the number of contaminated would have really exploded.

Even if the results are presented briefly in annex for the paper length sake, the model in t^m has also been applied with success to the hospitalized, with or without intensive care, and even to the deceased.

In order to better measure the contribution of the article, the proposed model in t^m is successively compared to two known models having the same number of parameters, namely a "convexity model" and a "convexity and concavity model", the Verhulst model, which has been rewritten under the form of a model in m^t so as to introduce a duality with the proposed model. The comparison is eloquent, in the sense that a quick analysis of the comparative illustration of the representativity of the models, clearly proves to be in favor of the model in t^m, whose representativity is better or more general according to the compared model.

Furthermore, in a context that scientifically involves complexity and simplicity, the self-filtering action of the internal structure, makes it possible to show the compatibility between the *internal complexity* (that the internal structure and its stochastic behavior present) and the *global simplicity* (that the deterministic model offers via its power-law t^m): it is true that the non-integer character of the power very simply expresses or represents complexity.

Appendix A. Impulse and step responses of non-integer integration operator and corresponding power-law

This appendix shows that the power-law, t^m, can be defined as the step response of a non-integer order integrator, or as the solution of a non-integer differential equation.

Impulse response

The unit impulse response, or response to the Dirac function, of the non-integer integration operator, of positive non-integer order, m, admits an expression of the form (Liouville (1832); Erdélyi (1962); Oustaloup (2014)):

$$y_{imp}(t) = \frac{t^{m-1}}{\Gamma(m)} u(t),$$

$u(t)$ being the Heaviside function and $\Gamma(m)$ the gamma function defined by:

$$\Gamma(m) = \int_0^\infty x^{m-1} e^{-x} dx.$$

Step response

The unit step response, or response to the Heaviside function, of the non-integer integration operator, of positive non-integer order, m, is given by the integral of the unit impulse response, namely, for $t > 0$:

$$y_{step}(t) = \int_0^t y_{imp}(\theta) d\theta,$$

or, given the expression of $y_{imp}(t)$:

$$y_{step}(t) = \int_0^t \frac{\theta^{m-1}}{\Gamma(m)} d\theta = \frac{1}{\Gamma(m)} \int_0^t \theta^{m-1} d\theta,$$

or else:

$$y_{step}(t) = \frac{1}{\Gamma(m)} \left[\frac{\theta^m}{m} \right]_0^t = \frac{1}{m\Gamma(m)} t^m = \frac{t^m}{\Gamma(m+1)},$$

a result that enables concluding that the step response (unit or not) of the integration operator of non-integer order, $m > 0$, well varies as the power-law t^m.

A non-integer differential equation governing the power-law t^m

Given the step response so obtained, the power-law t^m appears as a function $f(t)$ such that:

$$y_{step}(t) = \frac{f(t)}{\Gamma(m+1)},$$

or, in Laplace transforms:

$$Y_{step}(s) = \frac{F(s)}{\Gamma(m+1)} \quad \text{with} \quad F(s) = \mathcal{L}\left[f(t) = t^m\right],$$

a symbolic equation that enables writing, knowing that

$$Y_{step}(s) = \frac{1}{s^m} U(s) \quad \text{where} \quad U(s) = \mathcal{L}\left[u(t)\right]:$$

$$\frac{F(s)}{\Gamma(m+1)} = \frac{U(s)}{s^m},$$

namely:

$$s^m F(s) = \Gamma(m+1) U(s),$$

from where one draws the concrete equation:

$$\left(\frac{d}{dt}\right)^m f(t) = \Gamma(m+1) u(t),$$

a relation that expresses a linear differential equation of non-integer order, m, whose solution is nothing but the power-law $f(t) = t^m$.

Appendix B. Some applicative fields in which power-law dynamics occurs

Power-law dynamics such as expressed by t^m can be found in many applicative fields.

For example, in cosmology, the expansion of the universe is explained in Frieman et al. (2008) through the cosmic scale factor, $a(t)$, which is controlled by the dominant energy form $a(t) \propt t^{\frac{2}{3(1+w)}}$ for a constant w.

Also in fluid dynamics, the Tanner law, which was established in Tanner (1979) for explaining the spreading of silicone oil drops, enables explaining the spreading dynamics of fluid droplets according to $R(t) \propto t^m$ where $R(t)$ is the radius of the droplet (see Liang et al. (2009)).

And even in neurobiology, the dynamics of biological systems appear to be exponential over short-term courses and to be in some cases better described over the long-term by power-law dynamics. A model of rate adaptation at the synapse, between inner hair cells and auditory-nerve fibers, is presented in Zilany et al. (2009).

A non-exhaustive list of application fields that use the power-law dynamics, can be cited: in biochemical systems (Savageau (1970)), in DNA dynamics (Andreatta et al. (2005)), in semiconductor nanocrystals (Sher et al. (2008)), in water ressources (Harman et al. (2009)), in oscillators (Korabel et al. (2007)) and even in financial market (Gabaix et al. (2003)), etc.

Appendix C. Application of the FPM model to the official data on the hospitalized and the deceased

The proposed model in t^m, $A + Bt^m$, has also been applied with success to the hospitalized, with or without intensive care, and even to the deceased cases for the first two periods, that is to say the first convex period and the first concave one. The comparative evolutions are illustrated on figure C.18, where the official data are plot in solid lines, the models in the convex parts in circle symbols and the models in the concave parts are in star symbols. As expected, the provided models well fits the official data. Moreover, the parameters obtained after identification for the different models for each period are provided in table C.1, and the maximum relative error is provided, thus validating the proposed models.

References

Andreatta, D., Pérez Lustres, J. L., Pérez Lustres, J. L., Kovalenko, S. A., Ernsting, N. P., Murphy, C. J., Coleman, R. S., Berg, M. A., May 2005. Power-law solvation dynamics in dna over six decades in time. Journal of the American Chemical Society 127 (20), 7270—7271.

Arfan, M., Shah, K., Abdeljawad, T., Mlaiki, N., Ullah, A., 2020. A caputo power law model predicting the spread of the covid-19 outbreak in pakistan. Alexandria Engineering Journal.

Atangana, A., 2020. Modelling the spread of covid-19 with new fractal-fractional operators: Can the lockdown save mankind before vaccination? Chaos, Solitons & Fractals 136, 109860.

Battaglia, J.-L., Le Lay, L., Batsale, J.-C., Oustaloup, A., Cois, O., 2000. Heat flux estimation through inverted non integer identification models. International Journal of Thermal Science 39 (3), 374–389.

Chen, T., Rui, J., Wang, Q., Zhao, Z., Cui, J.-A., Yin, L., 2020. A mathematical model for simulating the transmission of wuhan novel coronavirus. bioRxiv.

De-Leon, H., Pederiva, F., 2020. Particle modeling of the spreading of coronavirus disease (covid-19). Physics of Fluids 32 (8), 087113.
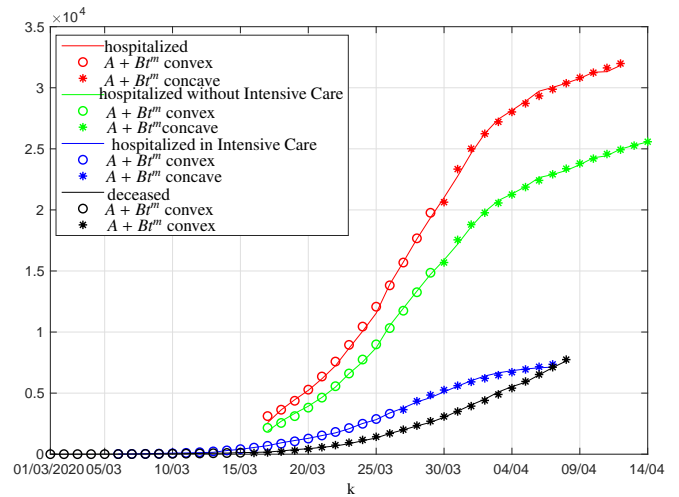
Figure C.18: Comparative evolution, during periods 1 and 2, of the hospitalized (—), hospitalized without intensive care (—), hospitalized in intensive care (—), and deceased (—) recorded by the Ministry and obtained with the models in t^m, one for the convex part (o) and one for the concave part (∗)

De Visscher, A., 2020. The covid-19 pandemic: model-based evaluation of non-pharmaceutical interventions and prognoses. Nonlinear Dynamics 101 (3), 1871–1887.

Dell'Anna, L., 2020. Solvable delay model for epidemic spreading: the case of covid-19 in italy. Scientific Reports 10 (1), 15763.

Demongeot, J., Griette, Q., Magal, P., 2020. Si epidemic model applied to covid-19 data in mainland china. medRxiv.

Efimov, D., Ushirobira, R., 2020. On interval prediction of covid-19 development based on a seir epidemic model. In: Journées Nationales Automtique de la SAGIP - Groupe de Travail Identification et COVID-19. Lille, France.

Erdélyi, A., 1962. Operational Calculus and Generalized Functions. Holt, Rinehart and Winston, New-York.

Ferguson, N. M., Cummings, D. A. T., Cauchemez, S., Fraser, C., Riley, S., Meeyai, A., Iamsirithaworn, S., Burke, D. S., 2005. Strategies for containing an emerging influenza pandemic in southeast asia. Nature 437 (7056), 209–214.

Frieman, J. A., Turner, M. S., Huterer, D., 2008. Dark energy and the accelerating universe. Annual Review of Astronomy and Astrophysics 46 (1), 385–432.

Gabaix, X., Gopikrishnan, P., Plerou, V., Stanley, H., 2003. A theory of power-law distributions in financial market fluctuations. Nature 423 (6937), 267–270.

Ganyani, T., Roosa, K., Faes, C., Hens, N., Chowell, G., 10 2018. Assessing the relationship between epidemic growth scaling and epidemic size: The 2014-16 ebola epidemic in west africa. Epidemiology and infection 147, 1–6.

Guan, L., Prieur, C., Zhang, L., Prieur, C., Georges, D., Bellemain, P., 2020. Transport effect of covid-19 pandemic in france. In: Journées Nationales Automtique de la SAGIP - Groupe de Travail Identification et COVID-19. Lille, France.

Harman, C. J., Sivapalan, M., Kumar, P., 2009. Power law catchment-scale recessions arising from heterogeneous linear small-scale dynamics. Water Resources Research 45 (9).

He, S., Peng, Y., Sun, K., 2020. Seir modeling of the covid-19 and its dynamics. Nonlinear Dynamics 101 (3), 1667–1680.

Huang, J., Qi, G., 2020. Effects of control measures on the dynamics of covid-19 and double-peak behavior in spain. Nonlinear Dynamics 101 (3), 1889–1899.

Huang, N. E., Qiao, F., Wang, Q., Tung, K.-K., 2020. Herd immunity vs suppressed equilibrium in covid-19 pandemic: different goals require different models for tracking. medRxiv.

Iacus, S. M., Santamaria, C., Sermi, F., Spyratos, S., Tarchi, D., Vespe, M., 2020. Human mobility and covid-19 initial dynamics. Nonlinear Dynamics

Table C.1: Identification parameters for the models in t^m of the hospitalized, hospitalized without intensive care, hospitalized in intensive care, and deceased for period 1 (convex part) and for period 2 (concave part)

Data	Dates	Part	k	m	A	B	mean (E_r)
hospitalized	17/03 − 29/03	convex part	1 − 13	1.6523	2876.401	243.8106	$-4.4\,10^{-4}$
	30/03 − 12/04	concave part	1 − 14	0.0964	−18558.02	39190.75	$1.4\,10^{-5}$
hospitalized without intensive care	17/03 − 29/03	convex part	1 − 13	1.6402	1956.690	191.9422	$-6.4\,10^{-4}$
	30/03 − 15/04	concave part	1 − 16	0.2572	6290.149	9504.363	$4.7\,10^{-6}$
hospitalized in intensive care	06/03 − 26/03	convex part	1 − 21	2.8455	14.7447	0.5692	$1.5\,10^{-2}$
	27/03 − 07/04	concave part	1 − 12	0.4078	1534.7680	2113.590	$1.0\,10^{-4}$
deceased	01/03 − 15/03	convex part	1 − 15	3.2097	3.1063	0.0200	$-3.9\,10^{-2}$
	16/03 − 09/04	convex part	1 − 27	1.9951	88.4450	13.5012	$3.8\,10^{-2}$

101 (3), 1901–1919.

Ivorra, B., Ferránez, M., Vela-Pérez, M., Ramos, A., 2020. Mathematical modeling of the spread of the coronavirus disease 2019 (covid-19) taking into account the undetected infections. the case of china. Communications in Nonlinear Science and Numerical Simulation 88, 105303.

Kermack, W., McKendrick, A., 1927. A contribution to the mathematical theory of epidemics. Proc. R. Soc. Lond A (115), 700–721.

Korabel, N., Zaslavsky, G., Tarasov, V., 2007. Coupled oscillators with power-law interaction and their fractional dynamics analogues. Communications in Nonlinear Science and Numerical Simulation 12 (8), 1405 – 1417.

Kwuimy, C. A. K., Nazari, F., Jiao, X., Rohani, P., Nataraj, C., 2020. Nonlinear dynamic analysis of an epidemiological model for covid-19 including public behavior and government action. Nonlinear Dynamics 101 (3), 1545–1559.

Kyurkchiev, N., Iliev, A., Rahnev, A., 2020. On the verhulst growth model with polynomial variable transfer. some applications. International. journal of differential, equations and applications 19 (1), 15–32.

Li, W., Zhou, J., Lu, J.-a., 2020. The effect of behavior of wearing masks on epidemic dynamics. Nonlinear Dynamics 101 (3), 1995–2001.

Liang, Z.-P., Wang, X.-D., Lee, D.-J., Peng, X.-F., Su, A., oct 2009. Spreading dynamics of power-law fluid droplets. Journal of Physics: Condensed Matter 21 (46), 464117.

Liouville, J., 1832. Mémoire sur quelques questions de géométrie et de mécanique et sur un nouveau genre de calcul pour résoudre ces équations. Journal de l'Ecole Polytechnique 13, 71–162.

Liu, X., Zheng, X., Balachandran, B., 2020. Covid-19: data-driven dynamics, statistical and distributed delay models, and observations. Nonlinear Dynamics 101 (3), 1527–1543.

Lu, Z., Yu, Y., Chen, Y., Ren, G., Xu, C., Wang, S., Yin, Z., 2020. A fractional-order seihdr model for covid-19 with inter-city networked coupling effects. Nonlinear Dynamics 101 (3), 1717–1730.

Mendes, G., da Silva, L., August 2009. Generating more realistic complex networks from power-law distribution of fitness generating more realistic complex networks from power-law distribution of fitness. Braz. J. Phys. 39 (2a).

Oustaloup, A., 1995. La dérivation non-entière : théorie, synthèse et applications. Hermès, Paris.

Oustaloup, A., 2014. Diversity and Non-integer Differentiation for System Dynamics. Wiley-ISTE.

Oustaloup, A., Levron, F., Mathieu, B., Nanot, F., 2000. Frequency-band complex noninteger differentiator: characterization and synthesis. IEEE Transactions on Circuits and Systems I: Fundamental Theory and Applications 47 (1), 25–39.

Rémond, J., Rémond, Y., 2020. Sur une modélisation simplifiée de l'épidémie du covid-19 de 2020, working paper or preprint.
    URL https://hal.archives-ouvertes.fr/hal-02551464

Richards, F., June 1959. A flexible growth function for empirical use. Journal of Experimental Botany 10 (29), 290–300.

Rohith, G., Devika, K. B., 2020. Dynamics and control of covid-19 pandemic with nonlinear incidence rates. Nonlinear Dynamics 101 (3), 2013–2026.

Roosa, K., Lee, Y., Luo, R., Kirpich, A., Rothenberg, R., Hyman, J. M., Yan, P., Chowell, G., 02 2020. Short-term forecasts of the covid-19 epidemic in guangdong and zhejiang, china: February 13-23, 2020. Journal of clinical medicine 9 (2), 596.

Santamaria, J., 2017. De la simplicité à la complexité. Le Monde. Voyage dans le cosmos.

Satsuma, J., Willox, R., Ramani, A., Grammaticos, B., Carstea, A., 2004. Extending the sir epidemic model. Physica A: Statistical Mechanics and its Applications 336 (3), 369 – 375.

Savageau, M. A., 1970. Biochemical systems analysis: Iii. dynamic solutions using a power-law approximation. Journal of Theoretical Biology 26 (2), 215 – 226.

Sher, P. H., Smith, J. M., Dalgarno, P. A., Warburton, R. J., Chen, X., Dobson, P. J., Daniels, S. M., Pickett, N. L., O'Brien, P., 2008. Power law carrier dynamics in semiconductor nanocrystals at nanosecond timescales. Applied Physics Letters 92 (10), 101111.

Tanner, L. H., 1979. The spreading of silicone oil drops on horizontal surfaces. Journal of Physics D: Applied Physics 12 (9), 1473–1484.

Tolle, J., 2003. Can growth be faster than exponential, and just how slow is the logarithm? The Mathematical Gazette 87 (510), 522–525.

Tuan, N. H., Mohammadi, H., Rezapour, S., 2020. A mathematical model for covid-19 transmission by using the caputo fractional derivative. Chaos, Solitons & Fractals 140, 110107.

Verhulst, P. F., 1838. Notice sur la loi que la population poursuit dans son accroissement. Correspondance mathématique et physique (10), 113–121.

Verhulst, P. F., 1845. Recherches mathématiques sur la loi d'accroissement de la population. Nouveaux mémoires de l'Académie Royale des Sciences et Belles-Lettres de Bruxelles 18, 14–54.

Viboud, C., Simonsen, L., Chowell, G., 2016. A generalized-growth model to characterize the early ascending phase of infectious disease outbreaks. Epidemics 15, 27 – 37.

Wang, X.-S., Wu, J., Yang, Y., 2012. Richards model revisited: Validation by and application to infection dynamics. Journal of Theoretical Biology 313, 12 – 19.

Wu, K., Darcet, D., Wang, Q., Sornette, D., 2020. Generalized logistic growth modeling of the covid-19 outbreak: comparing the dynamics in the 29 provinces in china and in the rest of the world. Nonlinear Dynamics 101 (3), 1561–1581.

Xu, C., Yu, Y., Chen, Y., Lu, Z., 2020. Forecast analysis of the epidemics trend of covid-19 in the usa by a generalized fractional-order seir model. Nonlinear Dynamics 101 (3), 1621–1634.

Zhao, S., Lin, Q., Ran, J., Musa, S. S., Yang, G., Wang, W., Lou, Y., Gao, D., Yang, L., He, D., Wang, M. H., 2020a. Preliminary estimation of the basic reproduction number of novel coronavirus (2019-ncov) in china, from 2019 to 2020: A data-driven analysis in the early phase of the outbreak. International Journal of Infectious Diseases 92, 214 – 217.

Zhao, Y.-F., Shou, M.-H., Wang, Z.-X., 06 2020b. Prediction of the number of patients infected with covid-19 based on rolling grey verhulst models. International journal of environmental research and public health 17 (12), 4582.

Zhou, X., Ma, X., Hong, N., Su, L., Ma, Y., He, J., Jiang, H., Liu, C., Shan, G., Zhu, W., Zhang, S., Long, Y., 2020. Forecasting the worldwide spread of covid-19 based on logistic model and seir model. medRxiv.

Zilany, M., Bruce, I., Nelson, P., Carney, L., 2009. A phenomenological model of the synapse between the inner hair cell and auditory nerve: long-term adaptation with power-law dynamics. Journal of the Acoustical Society of America 126 (5), 2390–2412.